

## The effect of atmospheric absorption of sunlight on the runaway greenhouse point

Toni Pujol and Joaquim Fort

Departament de Física, Universitat de Girona, Girona, Catalonia, Spain

Received 10 December 2001; revised 13 May 2002; accepted 12 June 2002; published 7 November 2002.

[1] The longwave emission of planetary atmospheres that contain a condensable absorbing gas in the infrared (i.e., longwave), which is in equilibrium with its liquid phase at the surface, may exhibit an upper bound. Here we analyze the effect of the atmospheric absorption of sunlight on this radiation limit. We assume that the atmospheric absorption of infrared radiation is independent of wavelength except within the spectral width of the atmospheric window, where it is zero. The temperature profile in radiative equilibrium is obtained analytically as a function of the longwave optical thickness. For illustrative purposes, numerical values for the infrared atmospheric absorption (i.e., greenhouse effect) and the liquid vapor equilibrium curve of the condensable absorbing gas refer to water. Values for the atmospheric absorption of sunlight (i.e., antigreenhouse effect) take a wide range since our aim is to provide a qualitative view of their effects. We find that atmospheres with a transparent region in the infrared spectrum do not present an absolute upper bound on the infrared emission. This result may be also found in atmospheres opaque at all infrared wavelengths if the fraction of absorbed sunlight in the atmosphere increases with the longwave opacity. *INDEX TERMS:* 3359 Meteorology and Atmospheric Dynamics: Radiative processes; 3309 Meteorology and Atmospheric Dynamics: Climatology (1620); 3346 Meteorology and Atmospheric Dynamics: Planetary meteorology (5445, 5739); 5407 Planetology: Solid Surface Planets: Atmospheres—evolution; 5409 Planetology: Solid Surface Planets: Atmospheres—structure and dynamics; *KEYWORDS:* atmospheric radiation limits, nongray atmospheres, greenhouse effect, antigreenhouse effect

**Citation:** Pujol, T., and J. Fort, The effect of atmospheric absorption of sunlight on the runaway greenhouse point, *J. Geophys. Res.*, 107(D21), 4566, doi:10.1029/2001JD001578, 2002.

### 1. Introduction

[2] *Simpson* [1927], *Komabayasi* [1967] and *Ingersoll* [1969] have investigated the greenhouse effect in atmospheres composed of a gas that equally absorbs radiation at all infrared wavelengths (i.e., gray atmosphere), transparent to sunlight and in equilibrium with its liquid (or solid) phase at the surface. In such atmospheres, the greenhouse effect is so intense that the outgoing longwave radiation (OLR) cannot exceed a given value (called SKI limit) and maintain the liquid (or solid) phase at the surface. A complete evaporation of the liquid (or solid) phase occurs when the OLR required to balance the absorbed sunlight exceeds the SKI limit. This runaway greenhouse effect is often used to explain the different evolution of the atmospheres of the terrestrial planets [e.g., *Curry and Webster*, 1999].

[3] The antigreenhouse effect arises from the absorption of sunlight by atmospheric gases or by haze layers optically thin to infrared radiation. This effect has been extensively analyzed in many planetary atmospheres as, for example, that found on Titan [*McKay et al.*, 1991; *Lorenz et al.*, 1997; *McKay et al.*, 1999] or on Earth in a nuclear winter scenario [*Turco et al.*, 1983].

[4] Our purpose is to qualitatively describe how the antigreenhouse effect modifies the runaway greenhouse point (i.e., the SKI limit). The gray assumption used in previous analytical studies [e.g., *McKay et al.*, 1999] appears inappropriate since the absorption of radiation by gases strongly depends on frequency. In addition, *Simpson* [1928] reveals the relevant role played by the gray absorption on the existence of the SKI limit. Therefore we include a transparent region in the spectrum of the infrared absorption (i.e., “semigray” atmosphere), crudely simulating the atmospheric “window” that appears in many gases (e.g., water vapor). The analytical solution for an atmosphere in radiative equilibrium only (i.e., neglecting convection) is introduced in section 2. Radiation limits for current Earth’s conditions are analyzed in section 3. Since we do not focus on a specific scenario, section 4 investigates the atmospheric radiation limits for a wide range of antigreenhouse parameters and for both gray and semigray greenhouse effects. Finally, the conclusions are presented in section 5.

### 2. Model Description

[5] We assume that a fraction  $1 - \gamma$  ( $0 \leq \gamma \leq 1$ ) of the net shortwave energy flux  $F_{SW}$  at top of the atmosphere (TOA) is not absorbed by the atmosphere, whereas the

atmospheric absorption of the remaining fraction  $\gamma$  exponentially decays with the shortwave optical depth  $t$ . Then the net absorbed shortwave energy flux  $F_{SW}(t)$  follows

$$F_{SW}(t) = (1 - \gamma)F_W(0) + \gamma F_{SW}(0)e^{-t}, \quad (1)$$

where  $t = 0$  corresponds to TOA.

[6] The shortwave optical depth at the surface is referred to as the shortwave optical thickness ( $\equiv t^*$ ). Since the intensity of the antigreenhouse effect increases with the atmospheric absorption of sunlight, high values of  $\gamma$  and  $t^*$  lead to strong antigreenhouse effects (see equation (1)). The steady state is reached when the outgoing longwave radiation equals the net shortwave flux at TOA (i.e.,  $OLR = F_{SW}(0)$ ).

[7] Temperature profiles for a fully transparent atmosphere to sunlight (first term in the rhs of equation (1)), and for a uniform exponential absorption of the solar beam (second term in the rhs of equation (1)) have been obtained by *Weaver and Ramanathan* [1995] in radiative equilibrium atmospheres with a non-gray greenhouse gas. These authors use a two-stream approximation to solve the transfer of the longwave radiation through the atmosphere. Due to the linearity of this approach, the solution for both heating at the surface and atmospheric extinction as in equation (1) is the sum of the individual solutions,

$$\begin{aligned} \sigma T^4(\tau) = & (1 - \gamma)F_{SW}(0) \frac{(1 + D\tau)}{2 + \beta D\tau^*} \\ & + \gamma F_{SW}(0) \left\{ \frac{2 + 3/\alpha + (\alpha - 3/\alpha)e^{-\alpha\tau}}{4(1 - \beta)} \right. \\ & \left. - \left[ \frac{2 + 3/\alpha + (2 - 3/\alpha)e^{-\alpha\tau^*}}{4(1 - \beta)(2 + \beta D\tau^*)} \right] \beta(1 + D\tau) \right\}, \quad (2a) \end{aligned}$$

$$\begin{aligned} \sigma T_g^4 = & (1 - \gamma)F_{SW}(0) \frac{(2 + D\tau^*)}{(2 + \beta D\tau)} \\ & + \gamma F_{SW}(0) \left[ \frac{2 + 3/\alpha + (2 - 3/\alpha)e^{-\alpha\tau^*}}{2(2 + \beta D\tau^*)} \right], \quad (2b) \end{aligned}$$

where  $T(\tau)$  is the atmospheric temperature at the longwave optical depth  $\tau$ ,  $\tau^*$  is the optical thickness (optical depth at the surface),  $\alpha$  is the ratio of the shortwave to the longwave optical depths (i.e.,  $\alpha = t / \tau$ ),  $\sigma$  is the Stefan-Boltzmann constant,  $T_g$  is the ground temperature,  $D = 3/2$ , and  $\beta$  ( $0 \leq \beta \leq 1$ ) is a measure of the effective width of the atmospheric window defined as

$$\beta = \frac{\int_{\lambda_l}^{\lambda_u} B_\lambda d\lambda}{\int_0^\infty B_\lambda d\lambda} \quad (3)$$

[*Weaver and Ramanathan*, 1995], where  $\lambda$  is the wavelength,  $B_\lambda$  is Planck's function and  $\lambda_l$  and  $\lambda_u$  are the lower and the upper limits of the transparent region in the infrared spectrum, respectively. In general,  $\beta$  is a function of temperature although equations (2a) and (2b) implicitly assume a constant value.

[8] Since the intensity of the greenhouse effect increases with the absorption of longwave radiation by the atmo-

sphere, high values of  $\beta$  (i.e., large window) lead to weak greenhouse effects. For a fixed value of infrared opacity  $\tau^*$ , the constant ratio of the shortwave to the longwave optical depths (or thickness)  $\alpha$  governs the shortwave optical thickness  $t^*$  used in the model. From the text below equation (1), large values of  $\alpha$  increase the antigreenhouse effect since the atmospheric opacity in the shortwave spectrum increases.

[9] Equations (2a) and (2b) with  $\beta = 0$  revert to the expressions for the antigreenhouse gray effect analyzed by *McKay et al.* [1999]. Note that the ground temperature  $T_g$  given by equation (2b) may differ from the air temperature at the surface  $T(\tau^*)$  (obtained from equation (2a) at  $\tau = \tau^*$ ). We also point out that the second term in the rhs of equation (2a) is slightly different in the work of *Weaver and Ramanathan* [1995] since these authors apply the two-stream approximation whereas we derive equations (2a) and (2b) from Eddington's approach [see, e.g., *Goody and Yung*, 1989].

[10] The semigray model detailed above appears more realistic than previous simple non-gray atmospheres used in the analysis of long-term atmospheric evolutions that ignored the temperature dependence on the longwave optical thickness [e.g., *Sagan and Mullen*, 1972; *Henderson-Sellers and Meadows*, 1976]. Here the optical thickness  $\tau^*$  in equations (2a) and (2b) depends on the mass absorption coefficient  $k$  and on the density of the absorbing gas  $\rho_a$ . *Ingersoll* [1969] shows from the liquid gas equilibrium condition that the optical thickness for both  $k$  and mass fraction  $\rho_a/\rho$  of the absorbing gas independent of height ( $\rho$  is the air density) follows

$$\tau^* = k \frac{p_s}{g} \frac{\rho_a}{\rho}, \quad (4)$$

where  $p_s$  is the surface pressure and  $g$  the acceleration of gravity. Equation (4) with  $\tau$  and  $p$  instead of  $\tau^*$  and  $p_s$  is often applied to the stratosphere (atmospheric layer in radiative equilibrium) [e.g., *Ingersoll*, 1969; *Nakajima et al.*, 1992].

[11] Since we neglect convective processes, the entire atmosphere in our simple model is in radiative equilibrium. Note that the atmospheric temperature (equation (2a)) in the gray case (i.e.,  $\beta = 0$ ) is independent of the optical thickness  $\tau^*$  and, hence, of the ground temperature  $T_g$ . Then, and for a gray atmosphere only, equation (2a) with (4) applied to the tropopause (intermediate level between the stratosphere and the convective layer below) may be understood as the tropopause temperature of a radiative-convective model.

### 3. Radiation Limits for Current Earth's Conditions

[12] Water vapor is the main absorbing gas of both shortwave and longwave radiation in current Earth's atmosphere. We assume that water vapor absorbs sunlight in the spectral band ranging from 0.55 to 2.5  $\mu\text{m}$  [see *Seinfeld and Pandis*, 1998]. It means that the fraction of the incoming shortwave radiation in this band is  $\gamma \approx 0.65$  (obtained from applying equation (3) to sunlight with a Sun's emission temperature equal to 5777 K). With this value of  $\gamma$ , and from equation (1), we obtain a shortwave optical thickness  $t^* \approx 0.98$  since

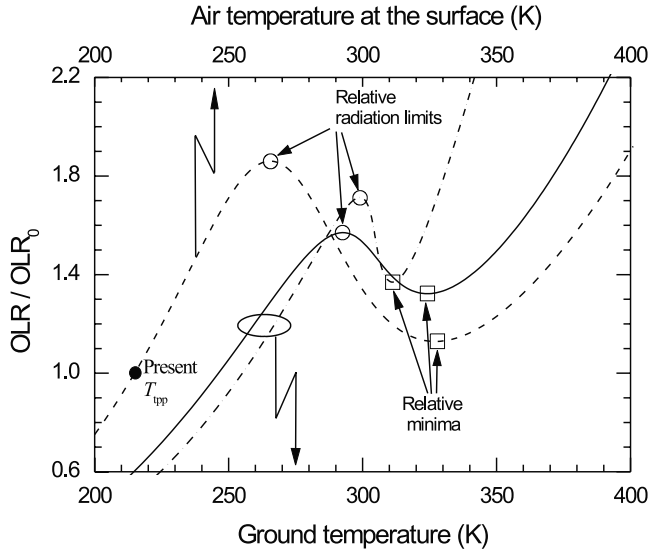


**Figure 1.** Outgoing longwave radiation OLR (normalized by its present Earth's value =  $240 \text{ W m}^{-2}$ ) as a function of atmospheric temperature at the surface  $T(\tau^*)$  and ground temperature  $T_g$ . The solid line corresponds to an atmosphere with water vapor as the main antgreenhouse gas ( $t^* = 0.98$ ;  $\gamma = 0.65$ ). The dash-dotted line is similar to the solid line but with a variable shortwave optical thickness  $t^*$  as a function of the longwave optical thickness  $\tau^*$  ( $\alpha = t^*/\tau^* = 0.25$ ;  $\gamma = 0.65$ ). The dashed line corresponds to an atmosphere with ozone as the main absorbing gas ( $t^* \rightarrow \infty$ ;  $\gamma = 0.03$ ). Note that our model atmosphere ignores convection, so that the air temperature at the surface may be understood as the tropopause value in a radiative-convective atmosphere (this is strictly valid in the gray version). Open circles and squares indicate relative maxima and minima, respectively. The closed circle indicates the tropopause temperature  $T_{tp}$  for present conditions ( $\text{OLR}/\text{OLR}_0 = 1$ ).

the net shortwave radiation at TOA  $F_{SW}(0)$  is  $240 \text{ W m}^{-2}$  and the absorption of sunlight in the atmosphere (i.e.,  $F_{SW}(0) - F_{SW}(t^*)$ ) is estimated to be about  $98 \text{ W m}^{-2}$  [see *Ozawa and Ohmura, 1997*]. Note that the  $t^*$  value above proposed overestimates the real shortwave optical thickness due to water vapor since other gases also contribute to absorb sunlight in the real Earth's atmosphere.

[13] The effective width of the atmospheric window in the infrared spectrum  $\beta$  ( $\approx 0.3$ ) is obtained from an average over terrestrial temperatures of equation (3) applied to a transparent region (i.e., region with a null absorption coefficient) ranging from  $\lambda_l = 8 \mu\text{m}$  to  $\lambda_u = 12 \mu\text{m}$  [see *Weaver and Ramanathan, 1995*]. The mean mass absorption coefficient for water vapor in the infrared spectrum outside the window is taken as  $k = 0.01 \text{ m}^2 \text{ kg}^{-1}$  [see *Ingersoll, 1969*].

[14] Water vapor is treated as a non-ideal gas. We use the fits to measured values given by *Irvine and Liley* [1983] for its density ( $\rho_a$ ) and partial pressure ( $p_v$ ) as a function of temperature. Since we assume the existence of liquid reservoirs at the surface (i.e., oceans), we apply the condition of saturation of the condensable greenhouse gas at  $\tau = \tau^*$ , from which  $\rho_a$  and  $p_v$  depend on temperature only [see *Irvine and Liley, 1983*]. Note that transport processes on current Earth's atmosphere prevent complete saturation at

the surface. Indeed, the globally averaged relative humidity observed at the surface is  $\approx 80\%$  [see *Manabe and Wetherald, 1967*]. Although the saturation condition could be relaxed by adding the relative humidity on the rhs of equation (4), next calculations assume full saturation of water vapor at the surface (i.e., relative humidity equal to 100%), a condition that gives a lower limit on the runaway greenhouse point. In addition to water vapor, dry air exerts a partial pressure at the surface equal to  $p_s = 1000 \text{ hPa}$  and it is treated as an ideal gas.

[15] Figure 1 shows the values of the air temperature at the surface  $T(\tau = \tau^*)$  and the ground temperature  $T_g$  as a function of the OLR (equal to  $F_{SW}(0)$  in stationary conditions) obtained from equations (2a) and (2b). The OLR in Figure 1 has been normalized by its present value ( $\text{OLR}_0 = 240 \text{ W m}^{-2}$ ). The vertical axis in Figure 1 may be understood as a non-linear axis in time since the flux coming from the sun (balanced with the OLR) increases with time from the theory of star evolution [e.g., *Crowley and North, 1991*] (we assume a constant planetary albedo).

[16] The solid line in Figure 1 refers to the ground temperature  $T_g$  and it uses the greenhouse  $\beta$  ( $\approx 0.3$ ) and antgreenhouse  $\gamma$  ( $\approx 0.65$ ) and  $t^*$  ( $\approx 0.98$ ) parameters detailed above. However, it is expected that the shortwave optical thickness  $t^*$  varies as a function of the longwave optical thickness  $\tau^*$  since water vapor is the main absorbing gas in the infrared as well as in the solar spectrum. The dash-dotted line in Figure 1 differs from the solid line by assuming a linear dependence of  $t^*$  on  $\tau^*$  with  $\alpha = t^*/\tau^* \approx 0.25$ . The value of  $\alpha$  has been obtained by using current Earth's atmospheric conditions ( $t^* \approx 0.98$ ,  $\tau^* \approx 4$ ) [see, e.g., *Thomas and Stamnes, 1999*].

[17] Note that ground temperatures  $T_g$  in Figure 1 for both solid and dash-dotted lines at  $\text{OLR}/\text{OLR}_0 = 1$  (i.e., current conditions) do not follow the observed value ( $T_g \approx 290 \text{ K}$ ). This is because most of the water vapor is found in the radiative-convective equilibrium layer of Earth's atmosphere (i.e., the troposphere). Convective processes in the troposphere sustain a critical lapse rate, which means that the vertical temperature profile does not follow the pure radiative equilibrium solution detailed in equation (2a). Ozone instead of water vapor is the main absorbing gas of sunlight at very high altitudes in the radiative equilibrium layer above the troposphere (i.e., in the stratosphere). Therefore we include the dashed line in Figure 1, which is a good analogue to Earth's radiative equilibrium layer. It depicts the normalized OLR as a function of the atmospheric temperature at the lower level of a pure radiative equilibrium atmosphere (i.e., equation (2a) at the surface) by assuming the values appropriate to the stratosphere, namely  $\alpha \rightarrow \infty$  (sunlight absorption at high altitudes),  $\gamma \approx 0.03$  (fraction of sunlight absorbed in the ozone layer) [see *Thomas and Stamnes, 1999*],  $\beta \approx 0.3$ , and saturation at the surface (i.e., water vapor saturated at temperature  $T_g$ ). Note that the result for present Earth's conditions ( $\text{OLR}/\text{OLR}_0 = 1$ ) is  $\approx 215 \text{ K}$  (see the closed circle), in agreement with observations of the tropopause temperature [e.g., *Hartmann, 1994*].

[18] The three results shown in Figure 1 present three different branches (i.e., sections with slopes of the same sign). From the theory of simple climate models, branches where  $T_g$  increases with OLR (positive slope) correspond to

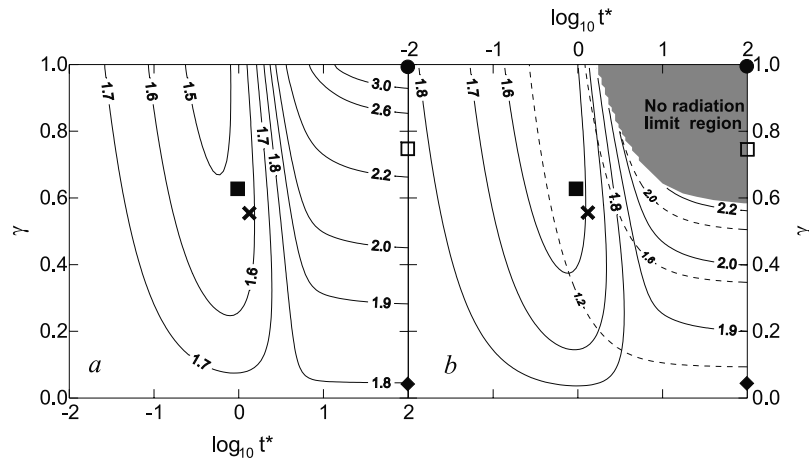


**Figure 2.** Radiation limits normalized by  $OLR_0$  ( $= 240 \text{ W m}^{-2}$ ) (solid contours) as a function of  $\gamma$  and  $t^*$  in (a) gray ( $\beta = 0$ ) and (b) semigray ( $\beta = 0.3$ ) atmospheres. The radiation limit in Figure 2a is absolute (SKI) whereas that in Figure 2b is relative. Dashed contours in Figure 2b refer to relative minima (see Figure 1). Symbols indicate values of the antigreenhouse parameters for current Earth’s stratospheric conditions (diamond), current Earth’s tropospheric conditions (closed square), early Earth’s (or Venus’) conditions (open square), current Venus’ conditions (circle), and current Titan’s state (cross).

stable climates, whereas branches with a negative slope refer to unstable, unattainable climates [see, e.g., *Rennó*, 1997]. An early Earth (low values of OLR) with an atmospheric composition similar to the present one would lie on the left stable branches depicted in Figure 1. As the solar flux increases, the planet may eventually reach the first bifurcation point (i.e., states with null slopes and indicated by open circles in Figure 1). This point is a relative radiation limit since, as mentioned above, negative-slope branches are unattainable [e.g., *Rennó*, 1997]. Therefore higher emissions would cause a jump of the planetary state into that point of the second stable branch with the same value of  $OLR/OLR_0$ . Note that in this branch the liquid vapor equilibrium condition still holds, in contrast to what happens in gray atmospheres, for which the maximum is absolute (SKI limit).

[19] The second stable branch for the three cases shown in Figure 1 does not have an absolute radiation limit (or SKI) because the existence of a fully transparent window in the infrared spectrum (i.e., of a  $\beta \neq 0$ ) does not constraint the maximum amount of longwave radiation that escapes to the space. States found in the second stable branch with  $OLR/OLR_0$  lower than the relative radiation limit are only attainable if the planet is initially in the second stable branch and the OLR emitted by the planet decreases with time. The hysteresis cycle of such a system as a function of the OLR, or equivalently  $F_{SW}(0)$ , is clear from the unattainability of the negative-slope branch. Indeed, if OLR decreased while at the high- $T$  stable branch, the jump to the low- $T$  stable branch would happen at the relative minima (open squares) shown in Figure 1.

[20] The stratospheric relative radiation limit shown in Figure 1 is  $\approx 1.86$  ( $\approx 446 \text{ W m}^{-2}$ ). It means that a radiative forcing on the order of  $206 \text{ W m}^{-2}$  at TOA would suffice to jump to the second warmer stable branch. Such a forcing would be reached at 5.5 Gyr from now by ignoring changes in both greenhouse and antigreenhouse parameters and by assuming the increase of solar luminosity on time only

[see *Caldeira and Kasting*, 1992]. However, the expected radiation limit obtained from radiative-convective models (not purely radiative ones) is  $\approx 1.3$  ( $\approx 310 \text{ W m}^{-2}$ ); [see *Kasting*, 1988; *Pierrehumbert*, 1995], which agrees with the expected timescale ( $\approx 2.5$  Gyr from now) for the loss of liquid water found in a complex biogeochemical model [see *Caldeira and Kasting*, 1992]. We point out that *Nakajima et al.* [1992] have shown that the radiation limit derived from radiative equilibrium conditions here investigated is an upper limit of the radiation limit imposed from radiative-convective equilibrium conditions.

#### 4. Sensitivity of the Radiation Limits to Antigreenhouse Parameters

[21] Here our purpose is to observe the influence of the antigreenhouse parameters on the atmospheric radiation limits. We consider first an atmosphere where the absorption of sunlight is independent of the infrared absorption. Then, not only  $\gamma$  but also  $t^*$  are independent of  $\tau^*$ . Figures 2a and 2b are contour plots of the radiation limit (normalized by  $OLR_0$ ) as a function of  $\gamma$  and  $t^*$  in gray (Figure 2a) and semigray (Figure 2b) atmospheres ( $\beta = 0.3$  in the latter case). Both panels have been obtained by plotting the analogue to Figure 1 (with  $\gamma$  and  $t^*$  independent of  $\tau^*$ ) and finding the extremes for each pair of values of  $\gamma$  and  $t^*$ . The fraction of sunlight absorbed in the atmosphere  $\gamma$  ranges from 0 to 1 (its maximum possible variation), and the optical depth for sunlight absorption  $t^*$  ranges from  $10^{-2}$  to 100 (expressed in a logarithm axis). Symbols in both panels indicate the antigreenhouse parameters associated with different atmospheres. The closed circle refers to present Earth’s conditions for water vapor as the main absorbing gas in the shortwave spectrum (i.e.,  $\gamma \approx 0.65$  and  $t^* \approx 0.98$ ; see the first paragraph in section 3). The closed diamond refers to present Earth’s stratospheric conditions, with ozone as the main absorbing gas of sunlight (i.e.,  $\gamma \approx 0.03$  and  $t^* \rightarrow \infty$ ; see the sixth paragraph in

section 3). The open square denotes early Earth's antigreenhouse parameters deduced from *Abe and Matsui* [1988], which are very similar to early Venus' values. The closed circle corresponds to present Venus' antigreenhouse parameters obtained from *Matsui and Abe* [1986]. Finally, the cross corresponds to present Titan's values from *Lorenz et al.* [1997, 1999].

[22] The radiation limit is absolute (i.e., it is a SKI limit) in Figure 2a. It means that for a given value of OLR (or, equivalently,  $F_{SW}(0)$ ) below the SKI limit, there is a single stable state (i.e., the warmer stable branches found in Figure 1 do not appear). Figure 2a clearly shows two different regions. For values of  $t^* > 3$ , the SKI limit largely varies with  $\gamma$ , reaching its maximum value at  $\gamma = 1$  (i.e., atmosphere with no transparent region in the shortwave spectrum). In this region, a higher SKI limit is obtained by increasing either  $\gamma$  or  $t^*$ , i.e., for a higher atmospheric absorption of shortwave radiation, as was intuitively expected (see also the text below equation (1)). In contrast, the SKI limit is almost independent of  $\gamma$  for  $t^* < 3$  (atmosphere optically thin to sunlight). On the other hand, we have found that both the temperature  $T_g$  and the longwave optical thickness  $\tau^*$  at the SKI limit increase as  $\gamma$  increases for any fixed value of  $t^*$ .

[23] A similar behavior is observed for the relative maxima (as open circles in Figure 1) shown as solid contours in Figure 2b. The dashed contours in Figure 2a represent the normalized relative minima (as open squares in Figure 1). The existence of the relative minimum implies a finite jump to the second stable branch when the OLR exceeds the relative radiation limit (see, e.g., Figure 1). The temperature change associated to this jump is smaller when the value of the solid line minus that of the dashed line is smaller. In a semigray atmosphere (i.e.,  $\beta \neq 0$ ), the antigreenhouse effect at high values of  $\gamma$  and  $t^*$  may eventually remove any radiation limit (Figure 2b). Thus the planet not only keeps the liquid phase for any value of OLR, but also evolves without any abrupt change in temperature for parameters of  $\gamma$  and  $t^*$  lying on the shaded region in the upper right corner in Figure 2b.

[24] Note that the relative maxima and minima found in Figure 2b for both diamond and closed square cases correspond to the limits shown in Figure 1 for both dashed and solid lines respectively. Surprisingly, the antigreenhouse parameters associated with early Earth and Venus cases (or, even, with the present Venus case) lie on the region without any radiation limit shown in Figure 2b. If we assume that the infrared window tends to close as surface temperature increases, the most reasonable result would correspond to the SKI limit found in Figure 2a. Nevertheless, the absolute radiation limit for these cases is also very high. For example, the SKI limit for early Earth (or early Venus) is  $\approx 2.3$  (see Figure 2a), whereas the maximum normalized outgoing longwave radiation would be equal to the normalized solar constant at early Venus orbit, being  $\approx 1.9$  ( $= 457.5 \text{ W m}^{-2}/240 \text{ W m}^{-2}$ ) only [see *Abe and Matsui*, 1988]. Thus this result removes the existence of a runaway effect in early Venus contradicting the planetary evolution suggested by several investigators [*Ingersoll*, 1969; *Rasool and de Bergh*, 1970; *Pollack*, 1971].

[25] Two possible explanations may resolve the apparent inconsistency of our previous results with the very likely

runaway process occurred in early Venus. The first one suggests that although the antigreenhouse parameters lead to a very strong antigreenhouse effect in the radiative equilibrium layer, the radiation limit determined from radiative-convective conditions may have reached a very small value (and below the net absorbed shortwave radiation). The second possible explanation is based on that the antigreenhouse parameters may depend on the amount of the greenhouse gas. This is obvious for a water vapor atmosphere as discussed in section 3. Note that not only  $t^*$  but also  $\gamma$  may vary as a function of  $\tau^*$ . Indeed,  $\gamma$  may increase by increasing the cloud-cover (or a hazy layer) and the cloud-cover may be a function of the surface temperature (i.e., of the longwave optical thickness). The present study ignores possible changes in the planetary albedo associated to variations in  $\gamma$ . However, we point out that this contribution would tend to increase the antigreenhouse effect since a priori the globally averaged cooling due to the albedo variation would prevail over the intensification of the greenhouse effect for an increase in cloud-cover (or in a haze layer).

[26] The expressions for  $t^* = t^*(\tau^*)$  and  $\gamma = \gamma(\tau^*)$  here employed follow  $t^* = \alpha \tau^*$  and  $\gamma = 1 - \exp(-G \tau^*)$  where both  $\alpha$  and  $G$  are positive constants. Note that both  $t^*$  and  $\gamma$  increase with  $\tau^*$ . The first expression has been used in the analysis of the greenhouse effect in gray atmospheres [see, e.g., *Goody and Yung*, 1989; *Ozawa and Ohmura*, 1997]. The second one has been applied to describe the effect on the shortwave absorption of the hazy layer at high altitudes found on Titan [see *Lorenz et al.*, 1999; *McKay et al.*, 1999]. For current Earth's conditions, and since water vapor is the main absorbing gas of both shortwave and longwave radiation, we find  $\alpha \approx 0.25$  and  $G \approx 0.26$  ( $t^* \approx 0.98$ ,  $\gamma \approx 0.65$ ,  $\tau^* \approx 4$ ; see section 3).

[27] Figures 3a and 3b show the relative radiation limit (solid line) and the relative minimum in OLR (dashed line), both normalized by  $OLR_0$ , as a function of  $\alpha$  and  $G$  for gray (Figure 3a) and semigray (Figure 3b) atmospheres ( $\beta = 0.3$  in the latter case). The solution for the gray atmosphere is, in essence, completely different to that obtained in Figure 2a. The radiation limits (solid lines) in Figure 3a are relative ones in contrast to the absolute SKI limits of Figure 2a. Note the region with no radiation limit in Figure 3a. This is of particular importance since some actual atmospheres may follow a semigray (i.e.,  $\beta \neq 0$ ) model at intermediate temperatures and a gray one (i.e.,  $\beta = 0$ ) at high temperatures. In water vapor atmospheres for example, the continuum absorption of water vapor increases the opacity of the atmospheric window when temperature increases [*Kasting*, 1988]. The behavior of the semigray atmosphere (Figure 3b) is similar to the gray one except with a larger region with no radiation limit and smaller changes in temperature when the atmosphere reaches the relative radiation limit and jumps to the second stable branch.

[28] Symbols in Figure 3 refer to the antigreenhouse parameters  $\alpha$  and  $G$  for the same cases described in Figure 2. We do not include the case for Earth's atmosphere with ozone as the main absorbing gas of sunlight since its amount is assumed to be almost independent of the main greenhouse parameter (water vapor). The relative radiation limit for current Earth's atmosphere from Figure 3 ranges

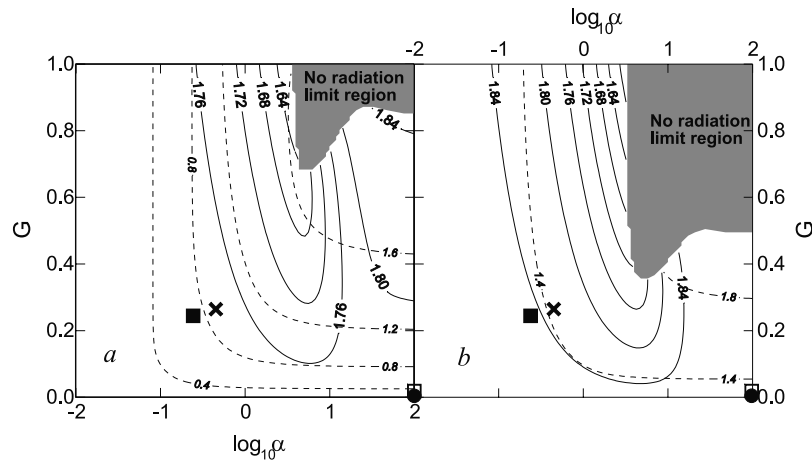


**Figure 3.** Radiation limits normalized by  $OLR_0$  ( $= 240 \text{ W m}^{-2}$ ) (solid contours) as a function of  $G$  and  $\alpha$  in (a) gray ( $\beta = 0$ ) and (b) semigray ( $\beta = 0.3$ ) atmospheres. ( $\gamma = 1 - \exp(-G\tau^*)$  and  $\alpha = t^* / \tau^*$ .) Dashed contours refer to relative minima. Symbols follow the antigreenhouse parameters detailed in Figure 2.

from 1.77 (gray case) to 1.84 (semigray case). Now, early Earth (or early Venus) conditions imply a relative radiation limit on the order of 1.78–1.85 (see the open square). These values are well below the maximum absorbed shortwave radiation at Venus’ orbit for early conditions ( $\approx 1.9$ ; see section 3). However, these values are above the maximum absorbed shortwave radiation at Earth’s orbit for early conditions ( $\approx 1.4 = 340 \text{ W m}^{-2}/240 \text{ W m}^{-2}$ ). This would suggest a finite runaway effect in early Venus but not in early Earth. Once in the second warmer stable branch, the amount of water vapor in the atmosphere would reach very high altitudes and eventually it might be lost by photodissociation due to its interaction with solar UV radiation.

[29] Note that Titan’s antigreenhouse parameters are depicted in Figures 2 and 3 for illustrative purposes only since its condensable greenhouse gas is not water vapor but both nitrogen and methane [see *Lorenz et al.*, 1999]. However, the qualitative behavior of the gas-liquid equilibrium curve for these gases is similar to that for water vapor. Then, Figure 3 may suggest that a multiple stable equilibrium as well as a finite runaway effect exist for this satellite, which is in close agreement with the findings of *Lorenz et al.* [1997, 1999] using specific models for Titan’s atmospheric structure.

## 5. Conclusions

[30] The SKI limit arises from a competition between the amount of absorber required by the liquid gas equilibrium condition (equation (4)) and that required by the emission of infrared radiation from the radiative equilibrium condition (equations (2a) and (2b)). We have investigated the effect of the atmospheric absorption of sunlight (antigreenhouse effect) on the SKI limit. Both gray and semigray greenhouse atmospheres have been analyzed. The semigray atmosphere uses a very schematic non-gray absorption in the infrared that crudely represents the atmospheric window observed for the water vapor. The main difference with previous analytical studies dealing with the SKI limit [e.g., *Nakajima et al.*, 1992] is the introduction of the antigreenhouse effect

in a semigray atmosphere (gray in studies by *Lorenz et al.* [1999] and *McKay et al.* [1999]).

[31] In this very simple model (mole fraction constant with altitude and no convective processes), the antigreenhouse effect is defined by the fraction of sunlight absorbed in the atmosphere  $\gamma$  and the shortwave optical thickness  $t^*$ . In some atmospheres, the infrared absorber may influence the shortwave absorption so  $\gamma$  and  $t^*$  may vary with the longwave optical thickness  $\tau^*$ .

[32] One of the two main results of the present paper is that the absolute radiation limit (SKI limit) disappears in a semigray atmosphere with a fully transparent window in the infrared. A relative radiation limit is found for weak to moderate values of the antigreenhouse parameters. It implies the possibility of a finite jump to the second stable (and not bounded) branch if the OLR exceeds the relative radiation limit. It also implies a multiple equilibrium (two different stable states for a given value of OLR) for OLR ranging from the relative minimum to the relative maximum (see, e.g., Figure 1). The relative radiation limit may eventually disappear for a very strong antigreenhouse effect (see Figures 2b and 3b). In this case, a single stable state is found for a given value of OLR.

[33] We stress that the temperature jumps, resulting from the multiple equilibria we have found, do not of course correspond to discontinuities of temperature versus time. Figure 1 corresponds to equilibrium states, but the system evolves through nonequilibrium transients. Thus the jump from the first to the second stable branch does not imply that the value of the temperature changes by a finite amount in an arbitrarily small time.

[34] Independently of the antigreenhouse parameters, the result for a semigray atmosphere with a fully transparent window in the infrared assures the liquid water equilibrium at any temperature. However, it does not remove the possible loss of water in the planet. Note that the amount of water vapor in the atmosphere increases with surface temperature. Then, it may eventually reach high altitudes in the atmosphere at very warm scenarios, where the interaction with UV radiation would

photodissociate water molecules with a subsequent escape of the hydrogen to space.

[35] The actual behavior of some atmospheres (as present Earth) would be better represented by an intermediate model between the gray and semigray cases since water vapor is not totally transparent within the window. At very warm scenarios, however, the atmospheric window in water vapor atmospheres would close due to the intense contribution of the continuum absorption [see, e.g., *Kasting*, 1988]. A gray rather than a semigray atmosphere would better simulate such a case.

[36] The second main result of the present paper is the complete change of the behavior found in gray atmospheres if the antigreenhouse parameters depend on the amount of the infrared condensable absorber. The radiation limit is absolute (SKI limit) for gray atmospheres with antigreenhouse parameters independent of the longwave absorbing gases (see Figure 2a), in agreement with *Ingersoll* [1969], *Nakajima et al.* [1992] and others. In contrast, the radiation limit may be relative for gray atmospheres with antigreenhouse parameters as a function of the infrared absorbing gases (see Figure 3a). In such a case, we also find a relative minimum in the OLR, which implies the possibility of a finite jump to the second not bounded stable branch if the OLR exceeds the relative radiation limit (similar to the result found for semigray atmospheres detailed above). This result agrees with previous analyses of Titan's atmosphere [see *Lorenz et al.*, 1997, 1999; *McKay et al.*, 1999]. For a very intense coupling between greenhouse and antigreenhouse parameters, the gray solution predicts a single stable state that holds the liquid phase equilibrium condition at any temperature below the critical point of the condensable gas (see the no radiation limit region in Figure 3a). This novel solution obtained for gray atmospheres does not necessarily remove the possible loss of water, as discussed above for the semigray atmosphere. We stress the importance of the new result found in gray atmospheres since the gray solution may be understood as the stratospheric solution for a radiative-convective model opaque in the infrared.

[37] For an Earth-like atmosphere in pure radiative equilibrium, the gray solution with a relative radiation limit (see the solid square in Figure 3a) is the most reasonable solution at high values of surface temperature. Current stratospheric conditions, however, are better represented with ozone antigreenhouse parameters in a gray atmosphere with an absolute (SKI) limit (see the diamond in Figure 2a). The normalized radiation limit (either relative or absolute) for both cases is on the order of 1.8, substantially greater than that obtained in radiative-convective models ( $\approx 1.3$ ) [*Kasting*, 1988; *Pierrehumbert*, 1995]. We point out that radiation limits derived from pure radiative equilibrium conditions refer to an upper bound since convective processes may reduce the SKI limit [see *Nakajima et al.*, 1992]. However, the values of the antigreenhouse parameters for early Earth and Venus conditions (see Figure 3) suggest a very likely runaway effect in early Venus, not found for early Earth conditions, in agreement with the expected planetary evolutions.

contract REN 2000-1621 CLI and by the Generalitat de Catalunya under grant SGR-2001-00186 (JF).

## References

- Abe, Y., and T. Matsui, Evolution of an impact-generated H<sub>2</sub>O-CO<sub>2</sub> atmosphere and formation of a hot proto-ocean on Earth, *J. Atmos. Sci.*, **45**, 3081–3101, 1988.
- Caldeira, K., and J. F. Kasting, The life span of the biosphere revisited, *Nature*, **360**, 721–723, 1992.
- Crowley, T. J., and G. R. North, *Paleoclimatology*, Oxford Univ. Press, New York, 1991.
- Curry, J. A., and P. J. Webster, *Thermodynamics of Atmospheres and Oceans*, Academic, San Diego, Calif., 1999.
- Goody, R. M., and Y. L. Yung, *Atmospheric Radiation: Theoretical Basis*, 2nd ed., Oxford Univ. Press, New York, 1989.
- Hartmann, D. L., *Global Physical Climatology*, Academic, San Diego, Calif., 1994.
- Henderson-Sellers, A., and A. J. Meadows, The evolution of the surface temperature of Mars, *Planet. Space Sci.*, **24**, 41–44, 1976.
- Ingersoll, A. P., The runaway greenhouse: A history of water on Venus, *J. Atmos. Sci.*, **26**, 1191–1198, 1969.
- Irvine, T. F., and P. E. Liley, *Steam and Gas Tables With Computer Equations*, Academic, San Diego, Calif., 1983.
- Kasting, J. F., Runaway and moist greenhouse atmospheres and the evolution of Earth and Venus, *Icarus*, **74**, 472–494, 1988.
- Komabayasi, M., Discrete equilibrium temperatures of a hypothetical planet with the atmosphere and the hydrosphere of one component-two phase system under constant solar radiation, *J. Meteorol. Soc. Jpn.*, **45**, 137–139, 1967.
- Lorenz, R. D., J. I. Lunine, and C. P. McKay, Titan under a red giant sun: A new kind of “habitable” moon, *Geophys. Res. Lett.*, **24**, 2905–2908, 1997.
- Lorenz, R. D., C. P. McKay, and J. I. Lunine, Analytic investigation of climate stability on Titan: Sensitivity to volatile inventory, *Planet. Space Sci.*, **47**, 1503–1515, 1999.
- Manabe, S., and R. T. Wetherald, Thermal equilibrium of the atmosphere with a given distribution of relative humidity, *J. Atmos. Sci.*, **24**, 241–259, 1967.
- Matsui, T., and Y. Abe, Impact-induced atmospheres and oceans on Earth and Venus, *Nature*, **322**, 526–528, 1986.
- McKay, C. P., J. B. Pollack, and R. Courtin, The greenhouse and antigreenhouse effects on Titan, *Science*, **253**, 1118–1121, 1991.
- McKay, C. P., R. D. Lorenz, and J. I. Lunine, Analytic solutions for the antigreenhouse effect: Titan and the early Earth, *Icarus*, **137**, 56–61, 1999.
- Nakajima, S., Y.-Y. Hayashi, and Y. Abe, A study on the “Runaway Greenhouse Effect” with a one-dimensional radiative-convective equilibrium model, *J. Atmos. Sci.*, **49**, 2256–2266, 1992.
- Ozawa, H., and A. Ohmura, Thermodynamics of a global-mean state of the atmosphere—A state of maximum entropy increase, *J. Clim.*, **10**, 441–445, 1997.
- Pierrehumbert, R. T., Thermostats, radiator fins, and the local runaway greenhouse, *J. Atmos. Sci.*, **52**, 1784–1806, 1995.
- Pollack, J. B., A nongrey calculation of the runaway greenhouse: Implications for Venus' past and present, *Icarus*, **14**, 295–306, 1971.
- Rasool, S. I., and C. de Bergh, The runaway greenhouse and the accumulation of CO<sub>2</sub> in the Venus atmosphere, *Nature*, **226**, 1037–1039, 1970.
- Rennó, N. O., Multiple equilibria in radiative-convective atmospheres, *Tellus, Ser. A*, **49**, 423–438, 1997.
- Sagan, C., and G. Mullen, Earth and Mars: Evolution of atmospheres and surface temperatures, *Science*, **177**, 52–56, 1972.
- Seinfeld, J. H., and S. N. Pandis, *Atmospheric Chemistry and Physics*, John Wiley, New York, 1998.
- Simpson, G. C., Some studies in terrestrial radiation, *Mem. R. Meteorol. Soc.*, **2**, 69–95, 1927.
- Simpson, G. C., Further studies in terrestrial radiation, *Mem. R. Meteorol. Soc.*, **3**, 1–27, 1928.
- Thomas, G. E., and K. Stamnes, *Radiative Transfer in the Atmosphere and Ocean*, Cambridge Univ. Press, New York, 1999.
- Turco, R. P., O. B. Toon, T. P. Ackerman, J. B. Pollack, and C. Sagan, Nuclear winter: Global consequences of multiple nuclear explosions, *Science*, **222**, 1283–1292, 1983.
- Weaver, C. P., and V. Ramanathan, Deduction from a simple climate model: Factors governing surface temperature and atmospheric thermal structure, *J. Geophys. Res.*, **100**, 11,585–11,591, 1995.

[38] **Acknowledgments.** This work has been partially funded by the Ministerio de Ciencia y Tecnología of the Spanish Government under

J. Fort and T. Pujol, Departament de Física, Universitat de Girona, Campus Montilivi, E-17071 Girona, Catalonia, Spain. (joaquim.fort@udg.es; toni.pujol@udg.es)